Electrochemical and Solid-State Letters, **5** (4) A67-A69 (2002)
0013-4651/2002/5(4)/A67/3/$7.00 © The Electrochemical Society, Inc.

Study of Membrane Degradation in High-Power Lithium-Ion Cells

Laura Norin,* Robert Kostecki,* and Frank McLarnon*,z

Lawrence Berkeley National Laboratory, Environmental Energy Technologies Division, Berkeley, California 94720, USA

Impedance spectra of Celgard® 2300 membranes that were removed from high-power Li-ion cells showed a significant rise in membrane ionic resistivity for cells that were cycled or stored at elevated temperatures. Atomic force microscopy images revealed dramatic changes in membrane surface morphology. Swelling of the membrane polypropylene fibers and the presence of particles of electrode active material in the membrane pores effectively reduced the membrane porosity, and thereby account for the membrane impedance rise and part of the cell power loss. These results not only indicate that membrane degradation can contribute significantly to Li-ion cell power loss at elevated temperatures, but also reveal mechanisms of membrane degradation.
 [DOI: 10.1149/1.1457206]

Manuscript submitted November 25, 2001; revised manuscript received January 6, 2002. Available electronically February 8, 2002.

The U.S. Department of Energy's Advanced Technology Development (ATD) program supports the development of high-power Li-ion batteries for hybrid electric vehicle applications.[1] Included in the ATD program are diagnostic evaluations of Li-ion cells that were aged and/or cycled under various conditions.[2] A primary goal of these diagnostic tests is to determine the mechanisms responsible for the cell power loss that accompanies life tests at elevated temperatures. Among the possible causes of power loss, degradation of the cell membrane and consequent reduced ionic conductivity is a mechanism that should be considered. However, studies of this mechanism in high-power Li-ion cells have not been reported in the literature.

Membrane porosity has been shown to be a determining factor for ion transport in batteries and fuel cells, limiting the cell current and reducing the ionic conductivity.[3-5] Studies have shown that storage at 75°C for 30 days increases the impedance of composite gel membranes by almost two orders of magnitude and that momentarily raising cell temperatures above the melting point of its polymer membrane produces equivalent effects on the membrane's electrical impedance.[6,7] Swelling of Nafion® membranes at elevated temperatures has also been documented.[8,9] No comparable studies on Celgard® 2300 membranes, which are commonly used in Li-ion batteries, have been reported; and none have expressly linked battery power loss with membrane impedance rise and structural instability. In fact, little attention has been paid to the possibility that membrane instability contributes to Li-ion cell power loss. In this study we focus on post-test analysis of Celgard 2300 membranes removed from high-power Li-ion cells which were stored and/or cycled at elevated temperatures. The effect of separator degradation on cell power loss is assessed.

Experimental

The high-power Li-ion cells included a $LiNi_{0.8}Co_{0.15}Al_{0.05}O_2$ cathode, a synthetic graphite anode, 1.2 M $LiPF_6$ + ethylene carbonate + ethylmethylcarbonate (EC/EMC) electrolyte, and a Celgard 2300 membrane separator. Membrane samples were taken from the following cells; (A) a fresh cell that was subjected only to formation cycles and initial characterization, (B) a cell that was at 60% state of charge (SOC) and shallow cycled at ±1.5% SOC for 4 weeks at 45°C and exhibited 10% power fade, and two cells which were stored at 60% SOC and 55°C for (C) 8 weeks and (D) 28 weeks. Cells C and D exhibited 14 and 24% power loss (power loss) respectively. The membranes of these cells were compared with unused Celgard 2300.

Impedance spectra were recorded inside an argon-filled glove box using a Solartron SI 1260 impedance phase analyzer and a Solartron SI 1286 electrochemical interface. Each sample had been soaked in electrolyte for 30 min prior to being placed between two identical 4.9 mm diam nickel electrodes. The electrodes were encased within a Teflon sheath, planed and polished to a mirror finish, and then set in a C-shaped stainless steel block. The lower electrode was fixed firmly in a cavity at the bottom of the "C" opening and was not moved during the experiments. The upper electrode was set loosely in a cavity at the top of the "C" opening. The upper electrode could be removed to allow insertion and removal of each membrane sample and to enable cleaning and rinsing of the electrodes with dimethyl carbonate before each test. During each test, the membrane was held between the electrodes at constant force, which was determined by the weight of the upper electrode. For each sample, impedance spectra were recorded at U_{ac} = 5 mV for ~12 different locations on the membrane.

Atomic force microscopy (AFM) images were recorded in contact mode using a Molecular Imaging Picoscan scanning probe microscope coupled with a ThermoMicroscopes Inc. AFM electronic controller. These measurements were carried out in open air on

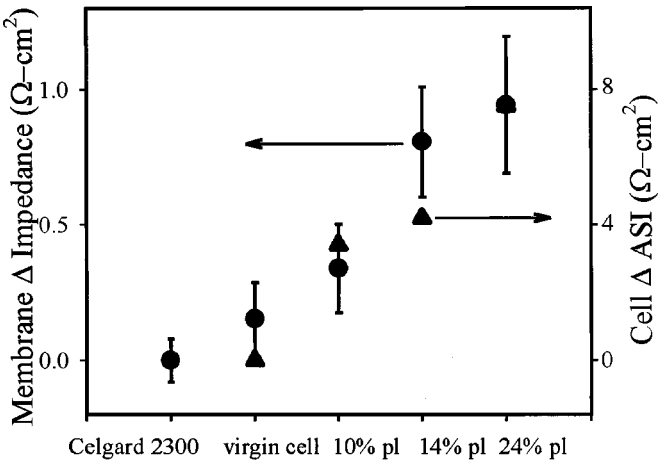

Figure 1. Left-hand ordinate and circles: change of Celgard 2300 membrane area-specific impedance, measured at U_{ac} = 5 mV and 80 kHz. Right-hand ordinate and triangles: change of Li-ion cell area-specific impedance, measured at 3.6 V after cell testing. (A) virgin: fresh cell. (B) 10% pl: cell cycled at 45°C for 4 weeks. (C) 14% pl: cell stored at 55°C for 8 weeks. (D) 24% pl: cell stored at 55°C for 28 weeks. Measurements of the area-specific impedance of fresh Celgard 2300 (average value normalized to zero) are shown for comparison. Error bars are determined by repeating measurements ~12 times at various locations on the membranes.

* Electrochemical Society Active Member.
z E-mail: frmclarnon@lbl.gov

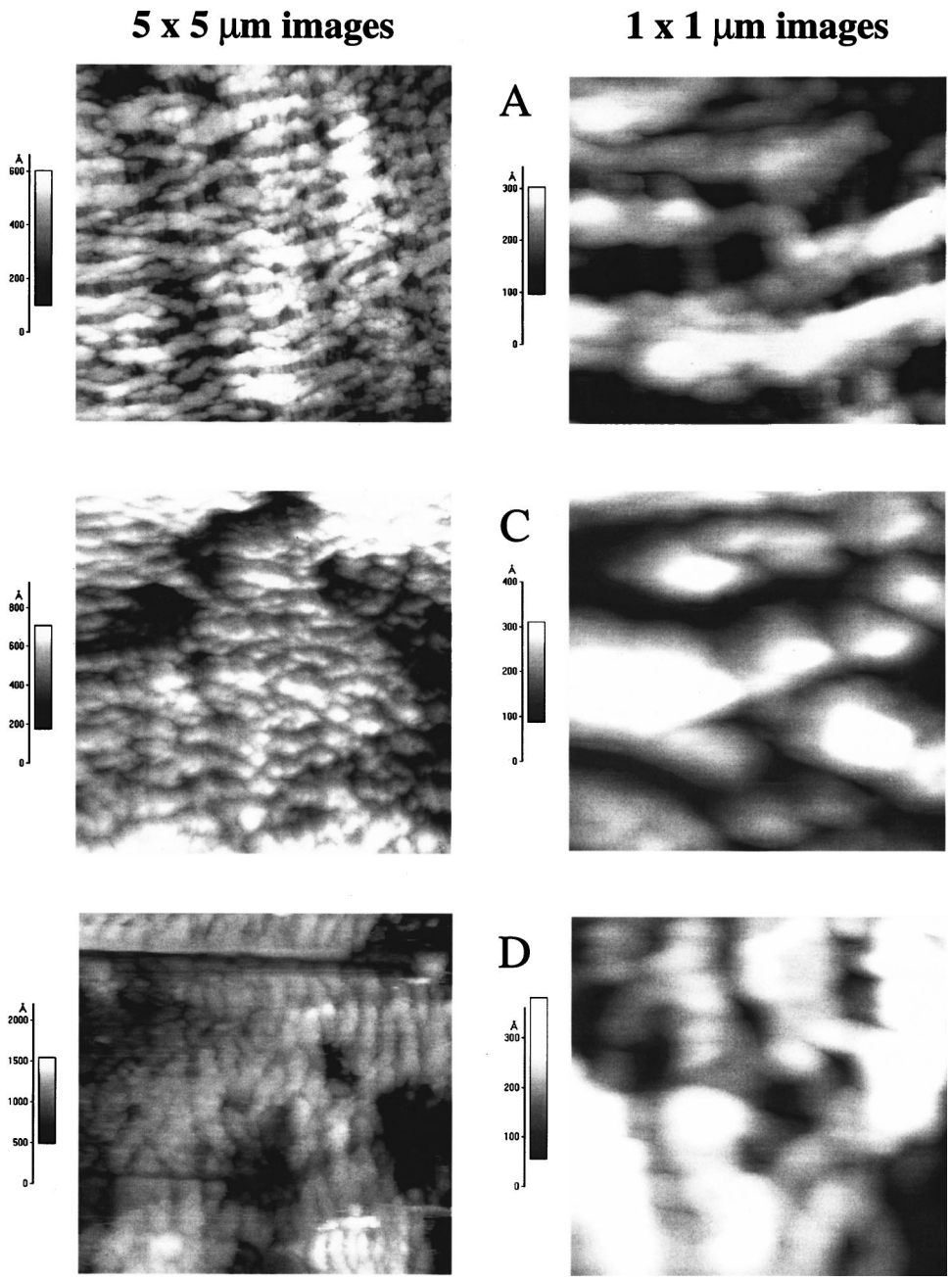

Figure 2. AFM images of the Celgard 2300 membranes extracted from (A) fresh cell, (C) cell stored at 55°C for 8 weeks, (D) cell stored at 55°C for 28 weeks. See the caption to Fig. 1 for additional detail.

membranes that had been washed in EMC prior to being removed from the glove box.

Labram, an integrated Raman microscope system provided by ISA Groupe Horiba, was used to analyze the structure of the membrane surfaces. The excitation wavelength was supplied by an internal 632 nm, 0.1 mW He-Ne laser.

Results

All impedance spectra displayed features characteristic of a series RC circuit at high frequencies. The membrane resistance was found by reading the real axis value at the high-frequency intercept, which occurred at ~80 kHz in all cases, and the results are plotted in Fig. 1. The change of membrane area-specific impedance (ASI), which reflects its reduced ionic conductivity, is plotted along with the corresponding change of Li-ion cell ASI (the latter was estimated from measurements of cell voltage drop upon current interruption at 3.6 V, before and after testing). It is clear that both cell cycling and aging, as well as the temperature at which the cell was stored, had a significant impact on the cell power loss and membrane impedance rise. The membrane from the fresh cell showed little impedance rise compared to unused Celgard 2300; however, the three aged and cycled membranes, B, C, and D, displayed impedance rises of 6, 21, and 25%, respectively. For membrane D, the area-specific impedance rise is about 1 Ω/cm^2. In comparison, the overall cell area-specific impedance rise for cell D was about 7 Ω/cm^2 at 60% SOC.

Note that the standard deviation error bars associated with the membrane resistance values widened significantly (*i.e.*, the local membrane resistance varied more strongly with position) with increasing average resistance. This result indicates that the membrane properties became more nonuniform as the cell aged. This phenomenon was particularly visible in membrane D, which exhibited local areas of dark coloration and high impedance due to contamination by detached electrode materials.

To investigate possible causes of the membrane impedance increase, AFM images of the membrane surfaces were recorded at

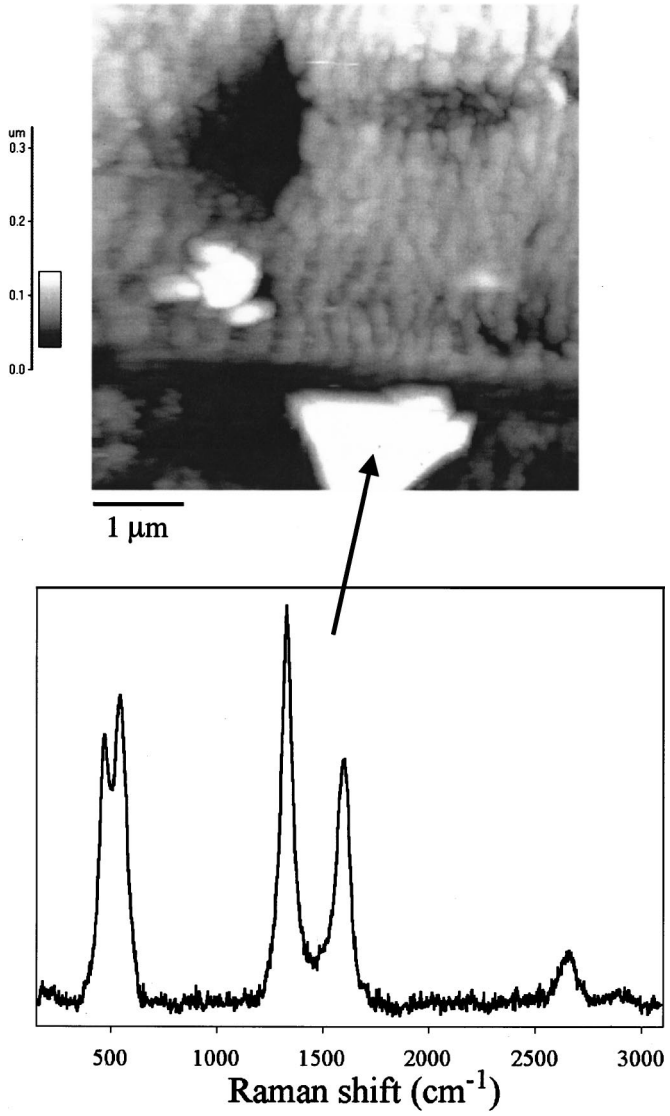

Figure 3. Upper panel: 5×5 μm AFM image of a contaminated area of the membrane from cell D (stored at 55°C for 28 weeks), which displayed high impedance. Lower panel: MicroRaman spectrum of a crystallite incorporated in the membrane from cell D; see text for a discussion of peak assignments.

various locations. Figure 2 shows typical 5×5 and 1×1 μm AFM images. The images of new Celgard 2300 (not shown) and the membrane from the fresh cell A were nearly identical. They consist of two layers of interwoven fibers arranged perpendicular to each other, presenting a regular structure of fibers and pores that allows ions to cross from anode to cathode. The membranes removed from either cycled or aged cells display dramatic changes in surface morphology. The polypropylene fibers appear swollen, and cracks and deep imprints from the grains of $LiNi_{0.8}Co_{0.15}Al_{0.05}O_2$ appear at the membrane surface. We believe that the increased fiber thickness is a result of swelling (possibly due to solvent penetration and reaction), rather than the deposition of a residue, because Raman spectroscopy measurements detected no new compounds covering the fibers (see below). This swelling significantly reduces both the size of the pores and the homogeneity of the membrane, thereby increasing the mean path length of the ions, and consequently increasing the potential drop across the membrane. This phenomenon may result in nonuniform current distribution across the cell and consequent accelerated electrode degradation at high-current locations. Membrane swelling can also increase mechanical stress in the cell, which may degrade electrode integrity.

Figure 3 shows a 5×5 μm AFM image of an area of membrane D with some dark gray coloration and high impedance. The bright area is a particle of cathode active material that separated from the cathode, became lodged in the membrane, and at least partially blocked a membrane pore. Raman microscopy spectra of these grains (a typical spectrum is shown in Fig. 3) show two peaks at 471 and 555 cm^{-1}, which are characteristic of delithiated $Li_{1-x}Ni_{0.8}Co_{0.15}Al_{0.05}O_2$. Because the cell was fully discharged before it was disassembled, the presence of charged material in the membrane suggests that either the electrode surface SOC was different than the bulk SOC (as implied by the presence of delithiated grains on the cathode surface) or the grains separated from the cathode earlier during cell testing. Two other peaks at 1330 and 1601 cm^{-1} correspond to carbon D and G bands, respectively. These peaks are characteristic of acetylene black, which was used as an additive in the $LiNi_{0.8}Co_{0.15}Al_{0.05}O_2$ cathode. We found traces of acetylene black in many areas of membrane D, a clear indication that carbon particles separated from the electrode in cell D.

Conclusions

We have demonstrated that Celgard 2300 membrane is at least partly unstable when used as a separator in high-power Li-ion cells with $LiPF_6$-EC-EMC electrolyte at elevated temperatures. The membrane impedance increases significantly upon cycling and/or aging of lithium-ion cells and accounts for ~15% of the total cell impedance rise. AFM images reveal swelling of polypropylene fibers and the presence of grains of cathode active material, which become lodged in the separator pores. The detailed mechanism of membrane degradation at elevated temperatures and its effect on the battery power loss should be investigated in greater detail.

Acknowledgments

This research was funded by the Assistant Secretary for Energy Efficiency and Renewable Energy, Office of Advanced Automotive Technologies, U.S. Department of Energy, under contract no. DE-AC03-76SF00098. The authors gratefully acknowledge the tested cells, help, and advice provided by the ATD Program participants.

Lawrence Berkeley National Laboratory assisted in meeting the publication costs of this article.

References

1. http://www.ott.doe.gov/pdfs/ATDFY2000ProgressReport.pdf
2. X. Zhang, P. N. Ross, Jr., R. Kostecki, F. Kong, S. Sloop, J. B. Kerr, K. Striebel, E. J. Cairns, and F. McLarnon, *J. Electrochem. Soc.*, **148**, A463 (2001).
3. F. G. B. Ooms, E. M. Kelder, J. Schoonman, N. Gerrits, J. Smedinga, and G. Calis, *J. Power Sources*, **97**, 598 (2001).
4. A. Magistris, P. Mustarelli, F. Parazzoli, E. Quartarone, P. Piaggio, and A. Bottino, *J. Power Sources*, **97**, 657 (2001).
5. G. Venugopal, J. Moore, J. Howard, and S. Pendalwar, *J. Power Sources*, **77**, 34 (1999).
6. G. B. Appetecchi, P. Romagnoli, and B. Scrosati, *Electrochem. Commun.*, **3**, 281 (2001).
7. F. C. Laman, M. A. Gee, and J. Denovan, *J. Electrochem. Soc.*, **140**, L51 (1993).
8. M. Doyle, M. E. Lewittes, M. G. Roelofs, S. A. Perusich, and R. E. Lowrey, *J. Membr. Sci.*, **184**, 257 (2001).
9. R. S. Yeo, *J. Appl. Polym. Sci.*, **32**, 5733 (1986).